

Tidal disruption events can power the observed AGN in dwarf galaxies

Kastytis Zubovas^{1,2,*}

¹*Center for Physical Sciences and Technology, Saulėtekio av. 3, Vilnius LT-10257, Lithuania*

²*Astronomical Observatory, Vilnius University, Saulėtekio av. 3, Vilnius LT-10257, Lithuania*

* *E-mail:* kastytis.zubovas@ftmc.lt

28 November 2018

ABSTRACT

In recent years, numerous active galactic nuclei have been discovered in ever smaller galaxies, questioning the paradigm that dwarf galaxies do not harbour central massive black holes. Even if such black holes exist, feeding them by gas streams is difficult, since star formation should be more efficient than AGN feeding in dwarf galaxies. In this paper, I investigate the possibility that tidal disruptions of stars are responsible for the observed AGN in dwarf galaxies. I show that the expected duty cycles of TDE-powered AGN, $f_{\text{AGN}} \gtrsim 0.5\%$, are consistent with observed AGN fractions assuming that the occupation fraction in dwarf galaxies is close to unity. Furthermore, I calculate the properties of outflows driven by TDE-powered AGN under idealised conditions and find that they might have noticeable effects on the host galaxies. Outflows themselves might not be detectable, except in gas-poor galaxies, where they can accelerate to $v_{\text{out}} > 100$ km/s, but increased gas turbulence, more diffuse density profile and lower star formation efficiency can be discovered and used to constrain the black hole occupancy fraction and more nuanced effects on dwarf galaxy evolution. If massive black holes form from seeds that are much more massive than stellar black holes, then their outflows should be easily detectable; this result, aided by observations of high-redshift dwarf galaxies, provides a potential way of determining seed masses of black holes.

Key words: galaxies: dwarf galaxies — galaxies: active — accretion, accretion discs — galaxies: evolution

1 INTRODUCTION

It is now generally well accepted that supermassive black holes (SMBHs) exist at the centres of all massive galaxies (Volonteri 2012; Graham 2016). Accretion energy released by SMBHs during the active galactic nucleus (AGN) phase, in the form of radiation, winds and jets, can have a significant impact on the morphology of the surrounding gas and star formation rate of the host galaxy (Shankar et al. 2006; McNamara & Nulsen 2007; Zubovas & King 2012; Zubovas et al. 2013), making them important elements of galaxy evolution. Recently, AGN have been detected in ever smaller galaxies (Greene et al. 2006; Pardo et al. 2016; Mezcua et al. 2016; Mezcua 2017; Mezcua et al. 2018), shrinking the mass gap between stellar and supermassive black holes. These discoveries suggest that AGN may have significant effects on dwarf galaxy evolution (see also Silk 2017) and provide potential ways of determining the occupation fraction and duty cycle of massive black holes in the low-mass range.

At first glance, it is difficult to see how SMBHs can be fed efficiently in dwarf galaxies. The short dynamical times there lead to rapid gas consumption by star formation and stellar feedback, starving the SMBH of fuel (Nayakshin et al. 2009). This argument explains the different scalings of central massive objects observed in galaxies with low and high central velocity dispersions (Ferrarese et al. 2006; Martin-Navarro & Mezcua 2018) and has been typically used as an explanation for the lack of SMBHs in dwarf galaxies. While some periods of activity are plausible simply due to stochastic variations in gas orbits, which can lead to gas streams occasionally feeding the SMBH efficiently, the duty cycle should be low enough that no significant SMBH growth should be expected in dwarf galaxies over a Hubble time. This conclusion is supported by recent results of Chilingarian et al. (2018); Bellovary et al. (2018), who find no correlation between the mass of 305 candidate intermediate mass black holes and host galaxy stellar masses.

On the other hand, SMBHs can potentially be fed by stellar tidal disruption events (TDEs). Each disruption event can easily feed the black hole in a dwarf galaxy at its Eddington rate for decades (Rees 1988; De Colle et al. 2012), and their cumulative effect may lead to noticeable growth. Previous research on the topic (Magorrian & Tremaine 1999; Wang & Merritt 2004; Stone & Metzger 2016) generally found that the smallest galaxies with SMBHs should have the highest rates of TDEs, because smaller galaxies are more compact and have shorter relaxation times (but see Brockamp et al. 2011). The total mass added to the SMBH by tidal disruption and direct swallowing of stars can reach $\sim 10^6 M_\odot$ over a Hubble time (Magorrian & Tremaine 1999), which can be a significant fraction of the SMBH mass at $z = 0$. The energy released during these disruption events can, in principle at least, drive outflows throughout the host galaxy.

In this paper, I investigate the importance of TDEs to the growth of SMBHs in dwarf galaxies. Using the TDE rates and their dependence on SMBH mass as derived by Stone & Metzger (2016), I find that SMBHs with seed mass $M_{\text{BH}}/M_\odot < 10^5$ can grow by $> 10\%$ over the Hubble time and are kept in an active state for 0.2 – 2.5% of the Hubble time by fuelling via TDEs only. This is consistent with observational results of AGN fraction in dwarf galaxies, assuming that most dwarf galaxies harbour central massive black holes. The energy released during these activity episodes can be several orders of magnitude higher than the gas binding energy of a gas-rich dwarf galaxy. Therefore, even wind-driven AGN outflows, with an energy coupling efficiency of $\eta \sim 5\%$, can have a noticeable effect on the host dwarf galaxy, even though the outflows themselves might be difficult to detect. Detection of dwarf galaxies perturbed by past AGN activity, combined with these results, would help determine the occupation fraction of massive black holes in dwarf galaxies and potentially help distinguish between massive black hole origin scenarios.

The paper is structured as follows. In Section 2, I review the argument as to why AGN feeding by gas flows should be inefficient in dwarf galaxies. In Section 3, I derive the expected mass growth and energy release caused by TDEs in SMBHs with different initial masses. In Section 4, I calculate the details of AGN outflow propagation and show that the impact on the host galaxy should be noticeable. In Section 5, I discuss the implications of these results. Finally, I summarize the results and conclude in Section 6.

2 FEEDING AGN IN DWARF GALAXIES WITH GAS STREAMS

Typically, nuclear activity is instigated by gas streams resulting from tidal disruption of molecular clouds falling close to the SMBH. A fraction of the cloud mass is captured by the SMBH gravitational potential and forms an accretion disc, which can feed the SMBH for periods of $10^4 - 10^5$ yr (King & Nixon 2015; Schawinski et al. 2015). However, the infalling gas can also form stars, and gas consumption by star formation and stellar feedback competes against SMBH feeding and feedback. Nayakshin et al. (2009) show, using analytical estimates based on relationships between luminosity, radius and velocity dispersion for large galaxies, that

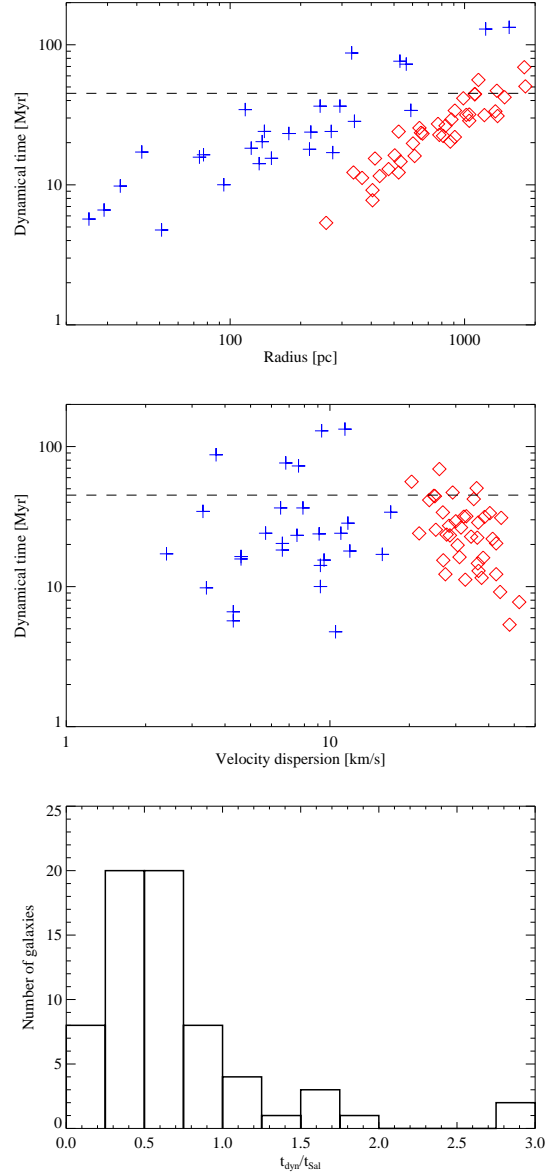


Figure 1. *Top:* Dynamical time against effective radius for dwarf galaxies in the Local group (blue crosses; Walker et al. 2009) and early-type dwarf galaxies in the Virgo cluster (red diamonds; Toloba et al. 2014). Dashed horizontal line shows $t_{\text{dyn}} = t_{\text{Sal}} = 45$ Myr. *Middle:* Dynamical time against velocity dispersion for the same galaxies. *Bottom:* Histogram of the ratio $t_{\text{dyn}}/t_{\text{Sal}} = t_{\text{dyn}}/(45\text{Myr})$ for the same galaxies.

in galaxies with central velocity dispersion $\sigma_* \lesssim 150 \text{ km s}^{-1}$, stellar feedback dominates over AGN feedback and the growth of the nuclear stellar cluster is more efficient than the growth of the SMBH. This argument is supported by results of numerical simulations (Finlator & Davé 2008; Schaye et al. 2010; Habouzit et al. 2017) and observations of a transition in the black hole mass - galaxy velocity dispersion relationship (Martin-Navarro & Mezcua 2018).

The same analytical argument can be applied to dwarf galaxies. Although they follow the baryonic Tully-Fisher relation $M_b \propto v^4$ (Iorio et al. 2017), with M_b the total baryon mass and v the circular velocity, the velocity dis-

persions exhibit a much larger scatter than typical for large galaxies (e.g., Kourkchi et al. 2012). Kinematical data of Local group dwarf spheroidals (Table 1 and references therein in Walker et al. 2009) shows only mild correlation between half-mass radius r_{half} and velocity dispersion σ , and essentially no correlation between dynamical time $t_{\text{dyn}} = r_{\text{half}}/\sigma$ and σ . However, only five of the 28 galaxies presented in that data set have $t_{\text{dyn}} > t_{\text{Sal}}$, where $t_{\text{Sal}} \simeq 45$ Myr is the Salpeter time. Similarly, only 4-6 out of 39 dwarf early-type galaxies in the Virgo cluster (Toloba et al. 2014) have $t_{\text{dyn}} > t_{\text{Sal}}$. In Figure 1, I show the relationship between t_{dyn} and effective or half-mass radius (top panel) and velocity dispersion (middle panel), as well as a histogram of the ratio $t_{\text{dyn}}/t_{\text{Sal}}$ (bottom panel), for these two dwarf galaxy samples. 84% of dwarf galaxies have dynamical times shorter than t_{Sal} , and 73% have $t_{\text{dyn}} < 0.75t_{\text{Sal}}$. Galaxies with $t_{\text{dyn}} > t_{\text{Sal}}$ are the largest in both samples, and it is certainly possible that dynamical times in their central regions, inside the sphere of influence of any putative central massive black hole, are significantly shorter.

Such approximate estimates suggest that SMBH feeding is less efficient than star formation in most dwarf galaxies. Gas falling in toward the centre of a dwarf galaxy is predominantly consumed by star formation, and stellar feedback disperses the gas more efficiently than AGN feedback. This conclusion is supported by observations of the correlation between star formation rate (SFR) and black hole accretion rate (BHAR). The ratio $\text{BHAR}/\langle \text{SFR} \rangle < 10^{-4}$ at $M_* \lesssim 10^{9.7} M_{\odot}$ (Yang et al. 2018) and potentially $\langle \text{BHAR} \rangle / \langle \text{SFR} \rangle < 10^{-4.5}$ at $M_* \lesssim 10^{8.2} M_{\odot}$ (Yang et al. 2017). The power of stellar wind feedback (Leitherer et al. 1992) is equal to AGN wind feedback power (King 2010) if $\langle \text{BHAR} \rangle / \langle \text{SFR} \rangle \simeq 3.5 \times 10^{-4}$ (Zubovas 2018, accepted), therefore low-mass galaxies should indeed be affected more strongly by stellar feedback than AGN feedback, at least on average. Another evidence in favour of this conclusion comes from numerical simulations of galaxy evolution, which show that black holes in dwarf galaxies are starved of gas (Bonoli et al. 2016; Trebitsch et al. 2017; Bellovary et al. 2018).

Stellar winds can in principle also feed AGN (e.g., Davies et al. 2012). If there is a star formation episode near the galactic nucleus, massive star winds may feed the AGN for several Myr afterward (Coker & Melia 1997; Cuadra et al. 2005; Davies et al. 2007; Cuadra et al. 2008). The feeding rate, however, is unlikely to be very large: Cuadra et al. (2005, 2008) find an expected rate of a few times $10^{-6} M_{\odot} \text{ yr}^{-1}$ for the conditions of the centre of the Milky Way. Assuming a radiative efficiency of 10%, this accretion rate corresponds to a bolometric luminosity of $L_{\text{bol}} \sim 10^{40} \text{ erg s}^{-1}$, close to the lower limit of detection for AGN in dwarf galaxies (cf. Mezcua et al. 2016, 2018, assuming a bolometric correction $B = 10$). In a dwarf galaxy, with a smaller nuclear star cluster and a smaller central black hole, the stellar wind accretion rate is likely to be much lower than the result of Cuadra et al. (2005).

Winds of low-mass main sequence or red giant stars can also feed the black hole (e.g., Shull 1983). The mass loss rate of a single red giant star can reach up to $10^{-4} M_{\odot} \text{ yr}^{-1}$ (Willson 2000). The wind capture rate by the SMBH is highly uncertain, however; as an upper limit, we may con-

sider the same simulations by Cuadra et al. (2008), where the black hole accretion rate is $\lesssim 0.3\%$ of the total mass injection rate by winds from massive stars well within the central parsec. The fraction drops by another factor ~ 2 when we consider that feedback outbursts can shut off accretion for extended periods of time (Cuadra et al. 2015). We can therefore estimate that a single red giant star in the star cluster around the SMBH feeds it at an average rate $\dot{M}_{\text{RG}} < 1.5 \times 10^{-7} M_{\odot} \text{ yr}^{-1}$. In order to feed a $10^5 M_{\odot}$ black hole at $\dot{M} = 0.01 \dot{M}_{\text{Edd}} = 2.2 \times 10^{-5} M_{\odot} \text{ yr}^{-1}$, there should be more than a hundred red giants in the surrounding nuclear star cluster, all emitting winds close to the peak rate. Since this peak mass loss rate cannot last for much longer than a few thousand years per star, this situation appears unlikely. As a more conservative estimate, we can consider the initial-final mass relations for stars of various masses and calculate that a stellar population loses $\sim 1/3$ of its initial mass via outflows from stars with $M_{\text{init}} < 8 M_{\odot}$ (Cummings et al. 2018). Considering a similar capture fraction as before, we see that only $\sim 10^{-3}$ of the nuclear star cluster mass will be added to the black hole mass over the cluster's lifetime. This fraction is negligible for any reasonable BH/cluster mass ratio. I therefore conclude that stellar winds are unlikely to contribute significantly to the growth of central black holes, although sporadic activity episodes may be generated by accretion of clumpy wind material.

3 TIDAL DISRUPTION AROUND IMBHs

3.1 TDEs as a power source for AGN

Even though, as shown in the previous section, AGN feeding by gas streams appears to be inefficient in dwarf galaxies, there is evidence that AGN feedback can affect the dwarf hosts (Penny et al. 2018). AGN feedback can potentially explain a large number of cosmological problems related to dwarf galaxies (Silk 2017). Therefore, it is interesting to consider tidal disruption events (TDEs) as a possible source of AGN fuel.

Typically, TDEs are considered only in terms of the flares with characteristic light curves, rather than significant contributors to the SMBH growth. However, the fallback rate of the disrupted material increases with decreasing SMBH mass, and exceeds the Eddington limit at $M_{\text{BH}} \leq 2.4 \times 10^7 M_{\odot}$ (De Colle et al. 2012). At lower masses, the phase of significant black hole feeding rate becomes ever longer. In particular, each TDE results in super-Eddington accretion for a time (Stone & Metzger 2016)

$$t_{\text{Edd}} = 5.1 \eta_{0.1}^{0.6} M_5^{-0.4} m_*^{0.2} r_*^{0.6} \text{ yr}, \quad (1)$$

where $\eta \equiv 0.1 \eta_{0.1}$ is the radiative efficiency of accretion, $M_5 \equiv M_{\text{BH}}/10^5 M_{\odot}$ is the BH mass, and m_* and r_* are the mass and radius of the disrupted star in Solar units.

During the super-Eddington fallback phase of the TDE, the flare luminosity is not directly proportional to the mass flow rate, because material builds up an accretion disc, which is then depleted on a viscous timescale, potentially powering an observable flare for $t > 100$ yr (Ramirez-Ruiz & Rosswog 2009; Hayasaki et al. 2013). During the super-Eddington accretion phase, the black hole behaves as a ULX, with luminosity varying as $L = L_{\text{Edd}} (1 + \ln(\dot{M}/\dot{M}_{\text{Edd}}))$

(Shakura & Sunyaev 1973; King & Lasota 2016). This results in a luminosity evolution $L \propto t^{-\alpha}$, where α varies between $\sim 1/4$ initially to the canonical value $5/3$ at late times, when the accretion rate drops below Eddington; however, Piran et al. (2015) argue that the flare is powered by energy release during the build-up of the accretion disc, which would lead to $L \propto t^{-5/3}$ at all times. In any case, the accretion disc can be expected to cool efficiently as long as $L > 10^{-2}L_{\text{Edd}}$ (e.g., Heckman & Best 2014), forming a geometrically thin disc and driving a wide-angle wind (King & Pounds 2003; King & Lasota 2016). This wind does not affect the disc feeding rate, since material falls on to the disc predominantly in the disc plane, but may affect the larger scale environment of the black hole.

The total energy released during a single TDE is uncertain. In the simplest picture, if approximately half of a Solar-mass star is eventually accreted with a 10% radiative efficiency, the expected energy release is of order 10^{53} erg; however, most observed TDEs have total energies 1-2 orders of magnitude lower (e.g., Gezari et al. 2012; Holoien et al. 2016; Eftekhari et al. 2018). This discrepancy may be explained if most of the energy is emitted in extreme UV (EUV), which is difficult to observe, or in jets beamed away from Earth (Lu & Kumar 2018). Alternatively, the disc wind may carry away a significant amount of mass and the total accreted mass may be only a small fraction of the initial mass of the disrupted star. In the following, I take the expression for the total radiated energy from Stone & Metzger (2016):

$$E_{\text{TDE}} = 2 \times 10^{51} \eta_{0.1}^{0.6} M_5^{0.6} m_*^{0.2} r_*^{0.6} \text{erg}, \quad (2)$$

which corresponds to an accreted mass

$$\Delta M_{\text{BH}} = \frac{E_{\text{TDE}}}{\eta c^2} = 1.1 \times 10^{-2} \eta_{0.1}^{-0.4} M_5^{0.6} m_*^{0.2} r_*^{0.6} M_{\odot}. \quad (3)$$

This is a conservative estimate, where only $\sim 1\%$ of the mass of the star ends up powering the TDE flare. In fact, the radiated energy estimate is $E_{\text{TDE}} \simeq L_{\text{Edd}} t_{\text{Edd}}$, but it may be significantly higher if we account for the buildup of the accretion disc during the super-Eddington feeding phase (Lin et al. 2017). Also, including the potential EUV emission increases the total energy, and hence the effect on the galaxy. In order to reduce possible uncertainties, I also do not account for the possibility of a phase of hyper-Eddington accretion, which may be relevant for black holes with $M \lesssim 8 \times 10^4 M_{\odot}$, which experience $\dot{M}_{\text{peak}} > 5000 \dot{M}_{\text{Edd}}$ (Inayoshi et al. 2016).

The goal of this paper is to provide a proof of concept that TDE-powered AGN can account for a significant part of the observed AGN population in dwarf galaxies, and that outflows caused by such AGN can have noticeable effects on the host galaxies. Therefore, I do not consider the precise details of individual TDEs, instead focusing on the conservative estimates for their numbers, durations and energy release.

3.2 TDE rates and properties in dwarf galaxies

There are significant uncertainties regarding the TDE rate and its dependence on host galaxy properties. It is generally expected that the TDE rate should be higher for lower-mass black holes (Wang & Merritt 2004; Stone & Metzger 2016);

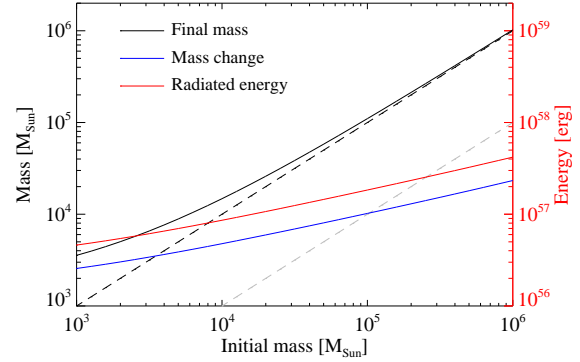


Figure 2. Expected growth of black holes over Hubble time via tidal disruption of stars. Black line show the initial-final mass relation, blue line shows the change in mass, red line shows the total radiated energy (scale on the right). Dashed black line shows a 1-to-1 correspondence between initial mass and final mass or mass change, grey dashed line shows 10% of the initial mass.

however, the scaling with BH mass may be opposite in star clusters (Sakurai et al. 2018). In particular, for cored galaxies, the expected TDE rate is (Stone & Metzger 2016)

$$\dot{N}_{\text{TDE}} = 6.6 \times 10^{-5} M_5^{-0.247} \text{yr}^{-1}. \quad (4)$$

The observed TDE rate is generally lower, of order $N_{\text{TDE,obs}} \sim 10^{-5} \text{yr}^{-1}$ per galaxy. Stone & Metzger (2016) provides an extensive discussion regarding the possible sources of this discrepancy. Mageshwaran & Mangalam (2018) provide a potential solution to the discrepancy, claiming that averaging the theoretically predicted results over the black hole mass function, and considering the detection probability of each event, leads to agreement between predicted and observed rates. In particular, the predicted rate, averaged over the galaxy population, can be a factor 2 higher than observed. Therefore, I will keep the estimate of eq. (4) for the rest of the calculations, and discuss the implications of it being lower in the Discussion section.

Combining equations (4) and (3) leads to an average mass growth rate over timescales much longer than $\dot{N}_{\text{TDE}}^{-1}$:

$$\dot{M}_{\text{BH}} = \dot{N}_{\text{TDE}} \Delta M_{\text{BH}} \simeq 7.3 \times 10^{-7} \eta_{0.1}^{-0.4} M_5^{0.353} m_*^{0.2} r_*^{0.6} M_{\odot} \text{yr}^{-1}. \quad (5)$$

Although mass growth via TDEs is stochastic and extremely bursty, the above expression can be used to estimate the total mass growth of the SMBH over the Hubble time. Rearranging the equation and integrating leads to an initial-final mass relation:

$$M_{f,5} = \left(M_{0,5}^{0.647} + 4.7 \times 10^{-3} \eta_{0.1}^{-0.4} m_*^{0.2} r_*^{0.6} \frac{t}{\text{Gyr}} \right)^{1.546}, \quad (6)$$

where $M_{0,5}$ and $M_{f,5}$ are the initial and final masses in units of $10^5 M_{\odot}$. Figure 2 shows this relation for initial masses $10^3 < M_0/M_{\odot} < 10^6$, as well as the difference between the two masses, assuming $\eta_{0.1} = m_* = r_* = 1$. As expected, the total mass gain is not very large, but can be significant for the smallest seed black holes. In particular, an $M_0 = 10^4 M_{\odot}$ black hole grows by a factor $M_f/M_0 \simeq 1.48$, while an $M_0 = 10^5 M_{\odot}$ one grows by only $\sim 10\%$.

The total energy released during TDEs over the Hubble

time is directly proportional to the mass change, i.e.

$$E_{\text{rad}} = \eta \Delta M c^2 = 1.8 \times 10^{53} \eta_{0.1} \text{erg} \frac{\Delta M}{M_{\odot}}. \quad (7)$$

This value is plotted as a red line in Figure 2, with scale on the right. We see that TDEs can result in release of $5 \times 10^{56} - 4 \times 10^{57}$ erg over the Hubble time. In the next section, I show that this energy release can have noticeable effect on the gas distribution in the host galaxy.

The duration of the TDE flare, in particular the super-Eddington phase (eq. 1), allows us to calculate the expected duty cycle of the AGN and the expected fraction of time for which the host galaxy is observed as being active. Using the standard TDE accretion rate relation $\dot{M} \propto t^{-5/3}$ (Rees 1988), which is applicable at late times at least (Lodato et al. 2009), we have that the duration for which the AGN is brighter than some threshold $L_{\text{thr}} < L_{\text{Edd}}$ is

$$t_{\text{thr}} = t_{\text{Edd}} \left(\frac{L_{\text{Edd}}}{L_{\text{thr}}} \right)^{3/5}. \quad (8)$$

Using this equation and the typical AGN threshold $L_{\text{AGN}} > 0.01 L_{\text{Edd}}$ (e.g., Heckman & Best 2014) gives

$$t_{\text{AGN}} \simeq 15.8 t_{\text{Edd}} \simeq 80.8 \eta_{0.1}^{0.6} M_5^{-0.4} m_*^{0.2} r_*^{0.6} \text{yr} \quad (9)$$

per TDE. The duty cycle is then

$$f_{\text{AGN}} = \dot{N}_{\text{TDE}} t_{\text{AGN}} \simeq 5.3 \times 10^{-3} \eta_{0.1}^{0.6} M_5^{-0.647} m_*^{0.2} r_*^{0.6}, \quad (10)$$

a value rather similar to the currently observed fraction of dwarf galaxies hosting AGN (0.4–3%, cf. Pardo et al. 2016; Mezcua et al. 2018). If, instead, a luminosity threshold is adopted, e.g. $L_X > 10^{41}$ erg s⁻¹ (Pardo et al. 2016), with a bolometric correction $L_{\text{bol}} \equiv 10 B_{10} L_X$, we have

$$f_{\text{AGN},X} = \dot{N}_{\text{TDE}} t_{\text{Edd}} \left(\frac{L_{\text{Edd}}}{B L_X} \right)^{3/5} \simeq 1.6 \times 10^{-3} \eta_{0.1}^{0.6} M_5^{-0.047} m_*^{0.2} r_*^{0.6} B_{10}^{-0.6}. \quad (11)$$

This value is somewhat smaller than current observational estimates. However, the threshold is somewhat subjective: using $L_X > 10^{39}$ erg s⁻¹ (following Mezcua et al. 2016, 2018), I find $f_{\text{AGN},X} = 0.025 \eta_{0.1}^{0.6} M_5^{-0.047} m_*^{0.2} r_*^{0.6} B_{10}^{-0.6}$, consistent with observed numbers.

Four effects can increase the expected duty cycle. First of all, more detailed modelling of fallback of material, including its self-gravity, shows that the disrupted gas stream can become clumpy and provide a higher peak fallback rate (Coughlin & Nixon 2015; Coughlin et al. 2016). Therefore, a larger fraction of TDEs might have prompt emission rising above the detection threshold. Furthermore, the super-Eddington fallback rate can persist for longer, by a factor ~ 1.5 , than given by simple analytical estimates (eq. 1; cf. Wu et al. 2018). Thirdly, if we assume that the falling material circularizes into a disc which then feeds the black hole via viscous transport, the duration of activity can extend even further, since the viscous timescale of a $10^5 M_{\odot}$ black hole is a few decades (Ramirez-Ruiz & Rosswog 2009). Such behaviour has been observed in super-Eddington TDEs (Lin et al. 2017), although currently the numbers are small and statistical analysis of their frequency and effects is difficult. Finally, the flaring rate may be somewhat higher if disruption of red giants is included.

3.3 Observable properties of TDE-powered AGN

These results suggest that TDE-powered AGN episodes may account for a significant fraction of all observed AGN in dwarf galaxies. As larger samples and longer-term observations of AGN in dwarf galaxies become available, it should be possible to distinguish TDE-powered episodes from other kinds of nuclear activity. This will allow for the testing of this prediction. In particular, the TDE-powered AGN flares should have certain properties that distinguish them from feeding via stellar winds or interstellar gas streams:

- The mass of the disrupted star is of order $M \sim 1 M_{\odot}$, while other kinds of gas streams do not have such a limitation; therefore, the mass of a TDE-fed accretion disc is always small, much smaller than the self-gravity limit $M_d \lesssim H/R M_{\text{BH}} \sim 10^{-3} M_{\text{BH}}$. This affects the AGN spectrum, since the luminosity of the disc, especially its outer regions, is likely to be smaller than in the case of a disc fed by gas streams.

- The disc feeding rate, and therefore also the disc mass, change significantly on timescales of years and decades. Even though at early times, neither the feeding rate nor the flare luminosity evolve as the classical estimate $\dot{M} \propto t^{-5/3}$ predicts, at late times this becomes true. Therefore, observations spanning multiple years and multiple dwarf AGN should find some AGN in the decay phase of their lightcurve. The upper limit to the fraction of AGN in the fading phase is

$$f_{\text{fade}} < \frac{t_{\text{AGN}} - t_{\text{Edd}}}{t_{\text{AGN}}} \simeq 0.94, \quad (12)$$

where t_{AGN} and t_{Edd} are taken from equations (9) and (1), respectively. Accounting for the super-Eddington disc feeding phase decreases this fraction, since the ‘plateau’ phase of the flare is extended by the viscous timescale of the accretion disc (Lin et al. 2017).

- In addition to changes on decade timescales, flares should show significant spectral variability on timescales much shorter than AGN fed by gas streams (Lin et al. 2017).

- Flares reach their peak luminosity very rapidly, on the orbital timescale of the bound disrupted material, therefore AGN in dwarf galaxies appearing abruptly would be better explained as TDEs rather than as being fed by gas streams.

While none of these properties can by itself identify TDE-powered AGN from those powered by gas streams, multiple lines of evidence may be used to distinguish between the two modes. If the TDE-powered AGN fraction among all dwarf galaxies turns out to be smaller than the estimates in equations (10) and (11), these results would also give another estimate of the massive black hole occupation fraction in dwarf galaxies. As the amount of data increases and our understanding of TDE properties grows, it should eventually be possible to determine the massive black hole occupation fraction in subsets of dwarf galaxies selected by mass or other properties. This would help significantly improve our understanding of the formation and growth of SMBHs throughout the Universe.

4 AGN OUTFLOWS IN DWARF GALAXIES

Independently of how an AGN is powered, its luminosity can have a significant effect on the host galaxy. If accretion proceeds via a thin disc, a disc wind can reach quasi-relativistic velocities $v_w \sim 0.1c$ and drive large-scale outflows which remove gas from the host galaxy (Zubovas & King 2012) and potentially trigger starbursts (Zubovas et al. 2013). In this section, I investigate the expansion of spherically-symmetric wind driven AGN outflows in dwarf galaxies using a 1D code and show that even AGN powered purely by tidal disruption of stars may have significant effects on their host galaxies. In TDEs, jets may have a similar energy output to disc radiation, but I do not include them in these calculations. I discuss the potential importance of jet feedback in Section 5.4.

4.1 Physical model

The wind outflow model is described in detail in King (2010) and Zubovas & King (2012). It is based on the observationally established fact that AGN accreting via a thin disc drive quasi-relativistic winds, which have velocities of order $v_w \sim 0.1c$ and mass flow rates \dot{M}_w comparable to the black hole accretion rate \dot{M}_{acc} (Pounds et al. 2003; Tombesi et al. 010a,b). Within the model, the wind self-regulates to keep an optical depth ~ 1 , which means that the photons of the AGN radiation field scatter on average once before escaping, and therefore

$$\dot{M}_w v_w = \frac{L_{\text{AGN}}}{c} = \eta \dot{M}_{\text{acc}} c. \quad (13)$$

As the wind reaches the interstellar medium (ISM), a two-shock system develops, with a forward shock driven into the ISM and a backward shock driven into the wind. If the backward shock cools efficiently, most likely via inverse-Compton scattering, most of the kinetic energy of the wind, $\dot{E}_w \simeq \eta L_{\text{AGN}}/2$, is radiated away and a momentum-driven outflow develops. Alternatively, if the wind doesn't cool, most of the energy is transferred to the ISM and an energy-driven outflow is formed. Cooling of the shocked wind is efficient only very close to the AGN (perhaps as close as $R_C < 1$ pc, cf. Faucher-Giguère & Quataert 2012), so the galaxy at large is affected by energy-driven outflows.

Assuming that the outflow is perfectly adiabatic and expanding in a spherically symmetric background potential, pushing a spherically symmetric gas distribution, the equation of motion is (for derivation see Zubovas & King 2016):

$$\ddot{R} = \frac{\eta L_{\text{AGN}}}{MR} - \frac{2\dot{M}\dot{R}}{M} - \frac{3\dot{M}\dot{R}^2}{MR} - \frac{3\dot{R}\ddot{R}}{R} - \frac{\ddot{M}\dot{R}}{M} + \frac{G}{R^2} \left[\dot{M} + \dot{M}_b + \dot{M} \frac{M_b}{M} - \frac{3}{2} (2M_b + M) \frac{\dot{R}}{R} \right]. \quad (14)$$

Here, $\dot{M} \equiv \dot{R} \partial M / \partial R$ and $\ddot{M} \equiv \ddot{R} \partial M / \partial R + \dot{R} (d/dt) (\partial M / \partial R)$. The first term on the right hand side is the driving term, the next four terms arise from the $p dV$ work and the kinetic energy of the outflow, and the terms in square brackets appear due to the force of gravity and work against the gravitational potential.

The assumption of spherical symmetry is, of course, a gross simplification of a real dwarf galaxy. A large fraction, perhaps the majority, of dwarf galaxies have irregular morphologies (Ann 2017). The TDE may be accompanied by

a jet which, by its nature, is a non-spherical phenomenon. Nevertheless, a spherically symmetric numerical model can give important insight into the processes happening in the system in question. In particular, one can obtain the typical outflow velocities and average velocities, pressures, as well as energy and momentum rates, which provide information on the expected observability of outflows, their escape from the galaxy and potential impact on star formation in the host. The expansion of outflows driven by wide-angle AGN winds and supernovae has been investigated extensively via 1D spherically symmetric numerical means (e.g., Sharma & Nath 2013; Zubovas & King 2016; Igarashi et al. 2017; Dashyan et al. 2018). In the Discussion section, I consider the possible effects of asymmetries in the gas distribution surrounding the black hole.

4.2 Numerical implementation

The equation of motion can be integrated numerically to provide all the salient outflow properties: $R(t)$, $v(t)$, $\dot{M}(t)$ and so on. I use a third order Taylor integration scheme with adaptive timesteps chosen according to the criterion $\Delta t = 0.1 \times \min\{R/\dot{R}, \dot{R}/\ddot{R}, \ddot{R}/\overset{\cdot}{\ddot{R}}, t_q\}$, where t_q is the AGN episode duration (see below). This integration preserves the adiabaticity of the system and recovers analytic solutions in idealised cases (Zubovas et al. 2011; Zubovas & King 2016) and only fails in situations where one or more parameters of the system change abruptly, but such situations only arise due to other assumptions in the model, such as perfect spherical symmetry.

In all the simulations presented here, the galaxy is defined by its total mass M_{tot} and a gas fraction $f_g \equiv M_g/M_{\text{tot}}$. The gas and underlying collisionless mass (dark matter and stars) is distributed in an NFW profile with parameters dependent on redshift z . Following Dutton & Macciò (2014), I adopt a relationship for concentration:

$$c = 10^{a+b \log(M_{12} h(z))}, \quad (15)$$

where

$$a = 0.52 + (0.905 - 0.52) \exp(-0.617z^{1.21});$$

$$b = -0.10 + 0.026z; \quad (16)$$

$$h(z) = h_0 (\Omega_\Lambda + \Omega_m (1+z)^3)^{1/2},$$

and, following Bryan & Norman (1998), a relation for the virial overdensity:

$$\Delta_{\text{vir}} = 18\pi^2 + 82x - 39x^2, \quad (17)$$

where

$$x = 0.308 \frac{(1+z)^3}{h(z)^2 / 0.678^2} - 1. \quad (18)$$

At each timestep, I update the redshift using the relation

$$\Delta z = -H_0 (1+z) (\Omega_\Lambda + \Omega_m (1+z)^3)^{1/2} \Delta t. \quad (19)$$

I use the most recent Planck cosmological parameters: $H_0 \equiv 100h_0 \text{ km s}^{-1} \text{ Mpc}^{-1} = 67.8 \text{ km s}^{-1} \text{ Mpc}^{-1}$, $\Omega_m = 0.308$, $\Omega_\Lambda = 0.692$ (Planck Collaboration et al. 2016).

At the centre of the gas distribution, I put an SMBH

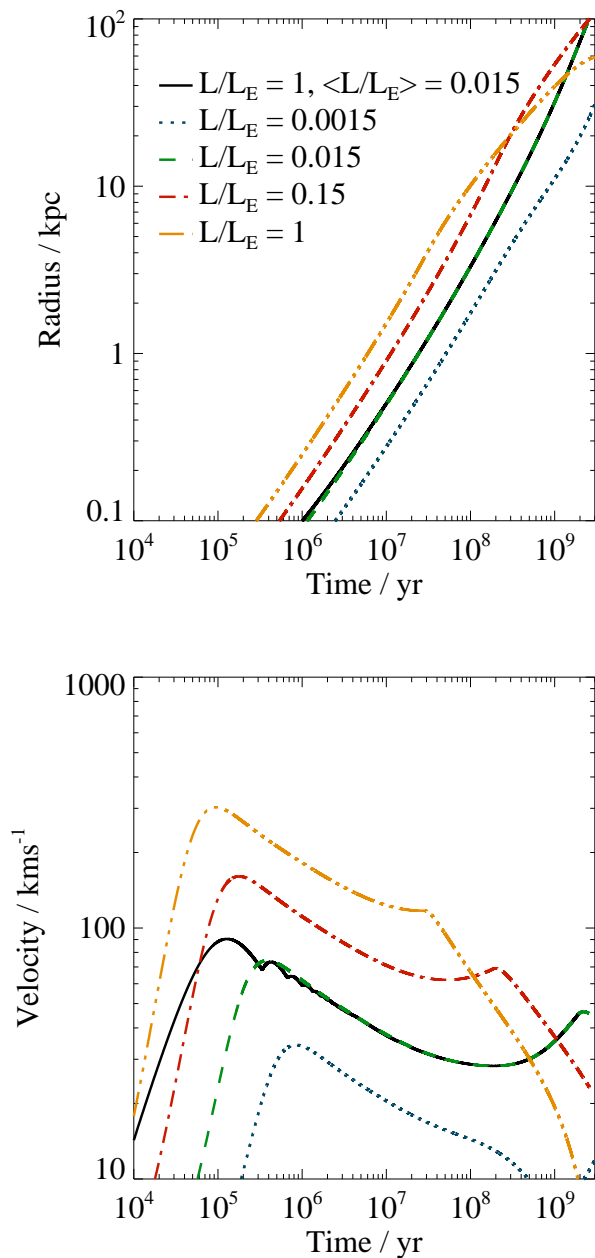


Figure 3. Outflow radius (top) and velocity (bottom) against time in simulations with bursty AGN luminosity history (black solid line) and several cases of continuous AGN activity, all limited by total energy output.

with mass M_{BH} . Nuclear activity is described by peak Eddington ratio $l = L_{\text{AGN}}/L_{\text{Edd}}(M_{\text{BH}})$ and episode duration t_q . All simulations begin at $z_{\text{init}} = 0.247$ and run for $t_{\text{tot}} = 3$ Gyr, giving the final $z_{\text{fin}} = 0$. The results do not change appreciably if the initial redshift is increased; I checked this with $z_{\text{init}} = 2$ and $z_{\text{init}} = 3$. This happens because the evolution of the halo parameters with redshift is rather weak.

4.3 Results

4.3.1 Bursty and continuous feedback

At first, I investigate the possible difference between long duration AGN episodes, such as would be caused by feeding of the SMBH via gas streams, and bursty feeding through TDEs. I choose a galaxy with total mass $M_{\text{tot}} = 3 \times 10^9 M_{\odot}$ with $f_g = 0.16$, i.e. $M_{\text{gas}} = 4.8 \times 10^8 M_{\odot}$, harbouring a central SMBH with $M_{\text{BH}} = 10^4 M_{\odot}$. I run five simulations in total. One has the BH experiencing Eddington-limited accretion episodes lasting $t_{\text{AGN}} = 5000$ yr every $t_{\text{rep}} = 0.33$ Myr, giving an average Eddington ratio $\langle l \rangle \simeq 0.015$. Although the values of both t_{AGN} and t_{rep} are much longer than those derived for TDE-powered AGN episodes, they still produce a large number of comparatively short AGN episodes, while allowing the simulation to run in reasonable time without using too much memory for storing the time evolution of outflow parameters. Four other simulations each have a single activity episode with $l = \{0.0015, 0.015, 0.15, 1\}$. AGN is shut off forever once the total energy released by the AGN reaches $E_{\text{tot}} = 1.15 \times 10^{57}$ erg. This is equivalent to the AGN injecting a kinetic energy $E_{\text{kin}} = 0.05 E_{\text{tot}} = 5.76 \times 10^{55}$ erg into the gas, which is 1.5 times the binding energy of the gas in the chosen potential. The switchoff time for the five simulations is $t_{\text{off}} = \{1.9, 18.7, 1.9, 0.19, 0.028\}$ Gyr; in the second simulation, $t_{\text{off}} > t_{\text{H}}$, so the AGN never switches off.

Figure 3 shows the propagation of outflows in these simulations. There are noticeable differences among the simulations with different Eddington ratios: simulations with brighter AGN produce faster outflows. Brighter AGN also produce more massive and energetic outflows. On the other hand, the fraction of AGN energy output converted to outflow kinetic energy is $\sim 2\%$ in all simulations, independently of the Eddington ratio. At late times, outflow radii in different simulations become more similar, suggesting that total injected energy is also an important parameter in determining the long-term outflow evolution.

The most important result can be seen by comparing the bursty simulation (black solid line) with the $l = 0.015$ simulation (green dashed line). Here, we see that burstiness has very little effect on outflow radius and velocity, except at very early times. Therefore it is the average Eddington ratio which determines the outflow properties. Motivated by this result, in subsequent simulations I use an average AGN luminosity, rather than bursty AGN luminosity history, to investigate outflows driven by TDE-powered AGN.

4.3.2 TDE-powered outflows

I now investigate the propagation of outflows in spherical potentials with parameters appropriate for dwarf galaxies. Given that a bursty activity history caused by TDEs is equivalent, for the purposes of outflow generation, to continuous activity with an appropriately reduced AGN luminosity, I choose an average AGN luminosity dependent only on its mass. Combining equations (5) and (7), this luminosity is

$$\langle L_{\text{AGN}} \rangle = \eta \dot{M}_{\text{BH}} c^2 = 4.2 \times 10^{39} \eta_{0.1}^{0.6} M_5^{0.353} m_*^{0.2} r_*^{0.6} \text{ erg s}^{-1}. \quad (20)$$

I consider galaxies with five values of total mass: $M_{\text{tot}} = 3 \times 10^8, 10^9, 3 \times 10^9, 10^{10}$ and $3 \times 10^{10} M_{\odot}$; the last mass exceeds

Model ID	M_{tot}/M_{\odot}	M_{gas}/M_{\odot}	$M_{\text{BH},0}/M_{\odot}$	E_{b}/erg	E_{SN}/erg	$E_{\text{AGN}}/\text{erg}$	$E_{\text{b}}/E_{\text{AGN}}$	$E_{\text{SN}}/E_{\text{AGN}}$
M3e8	3×10^8	4.79×10^7	34	3.3×10^{53}	1.2×10^{54}	2.8×10^{56}	1.2×10^{-3}	4.3×10^{-3}
M1e9	10^9	1.59×10^8	200	2.4×10^{54}	7.1×10^{54}	3.3×10^{56}	7.3×10^{-3}	0.022
M3e9	3×10^9	4.76×10^8	980	1.5×10^{55}	3.5×10^{55}	4.4×10^{56}	0.034	0.080
M1e10	10^{10}	1.58×10^9	6.2×10^3	1.1×10^{56}	2.2×10^{56}	7.2×10^{56}	0.15	0.31
M3e10	3×10^{10}	4.69×10^9	3.1×10^4	7.1×10^{56}	1.1×10^{57}	1.2×10^{57}	0.59	0.92
M3e8-lowfg	3×10^8	1.2×10^5	34	9.0×10^{50}	1.2×10^{54}	2.8×10^{56}	3.2×10^{-6}	4.3×10^{-3}
M1e9-lowfg	10^9	7.1×10^5	200	1.2×10^{52}	7.1×10^{54}	3.3×10^{56}	3.6×10^{-5}	0.022
M3e9-lowfg	3×10^9	3.5×10^6	980	1.2×10^{53}	3.5×10^{55}	4.4×10^{56}	2.7×10^{-4}	0.080
M1e10-lowfg	10^{10}	2.2×10^7	6.2×10^3	1.7×10^{54}	2.2×10^{56}	7.2×10^{56}	2.4×10^{-3}	0.31
M3e10-lowfg	3×10^{10}	1.1×10^8	3.1×10^4	1.8×10^{55}	1.1×10^{57}	1.2×10^{57}	0.015	0.92

Table 1. Parameters of TDE-powered AGN outflow simulations. First column shows model ID, the next four columns give the total mass, baryon fraction, gas mass and initial mass of central BH. The final three columns give the gas binding energy, the expected energy from SN explosions over the Hubble time, and the expected energy release by the AGN over the Hubble time.

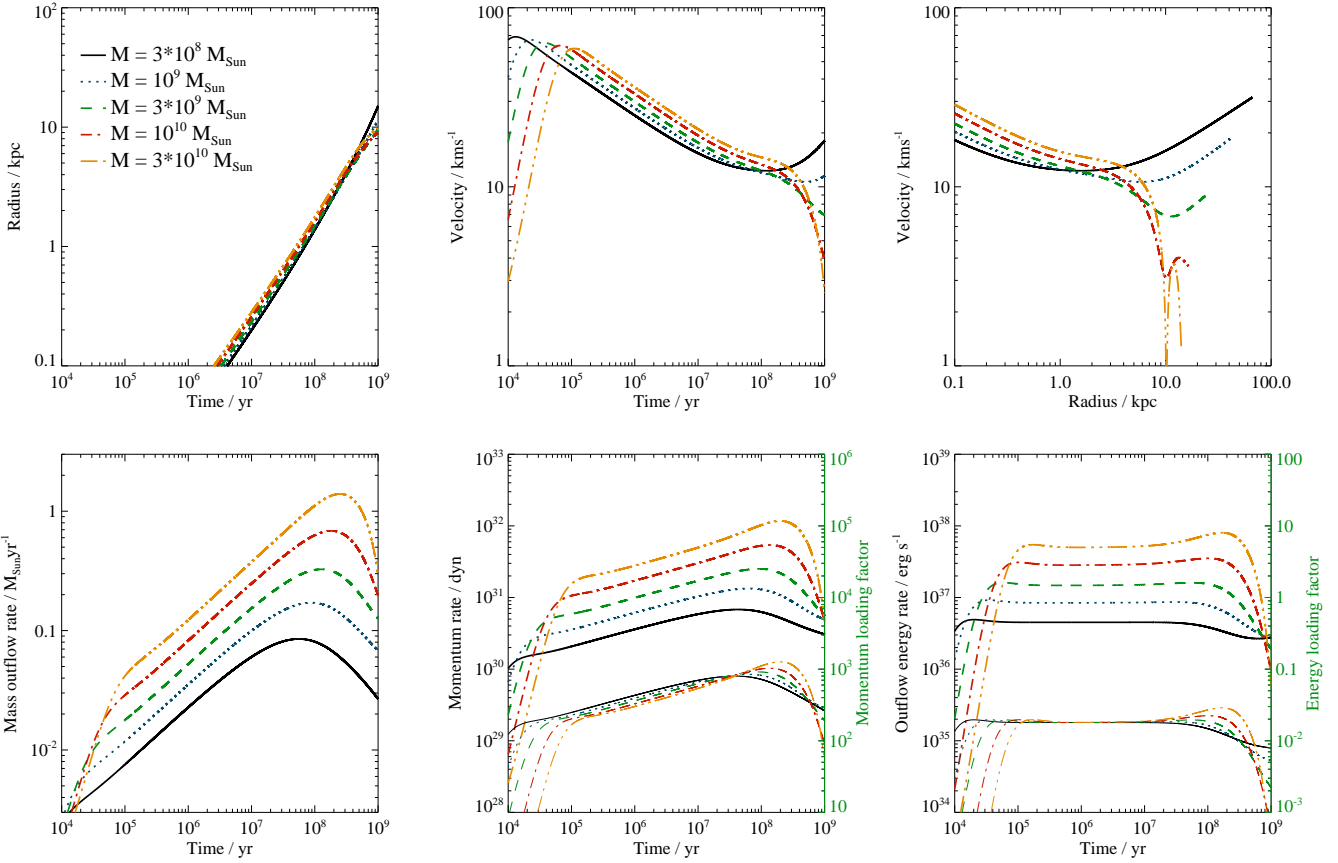


Figure 4. Outflow parameters in simulations with TDE-powered AGN, starting at $z_{\text{init}} = 0.247$, with BH masses linearly proportional to stellar masses and baryon fraction $f_{\text{b}} = 0.16$. *Top left:* outflow radius against time. *Top middle:* outflow velocity against time. *Top right:* outflow velocity against radius. *Bottom left:* mass outflow rate against time. *Bottom middle:* outflow momentum rate (thick lines) and momentum loading factor $\dot{p}_{\text{out}c}/\{L_{\text{AGN}}\}$ (thin lines). *Bottom right:* outflow kinetic energy rate (thick lines) and energy conversion efficiency $\dot{E}_{\text{kin}}/\{L_{\text{AGN}}\}$ (thin lines). The five lines correspond to models with different total masses (see Table 1 and text for details).

that of the LMC ($M_{\text{LMC}} \leq 3 \times 10^{10} M_{\odot}$; van der Marel et al. 2002; Kallivayalil et al. 2006). The present-day stellar mass M_{\star} is taken from the abundance matching relation in Read et al. (2017), giving $M_{\star}(z=0) = 1.2 \times 10^5, 7.1 \times 10^5, 3.5 \times 10^6, 2.2 \times 10^7$ and $1.1 \times 10^8 M_{\odot}$ for the five values of total mass. I further assume that $M_{\star}(z=0.247) = M_{\star}(z=0)$, i.e. that no significant star formation occurred

in these galaxies for the past 3 Gyr. This is approximately correct for dwarf spheroidal and elliptical galaxies in the Local Group (Weisz et al. 2014).

I consider two possible values of gas mass in the galaxy, leading to 10 models in total. In one group of models, I assume a baryon fraction $f_{\text{b}} = 0.16$ and take $M_{\text{gas}} = f_{\text{b}} M_{\text{tot}} - M_{\star}$. This gives an upper limit to the gas mass, since

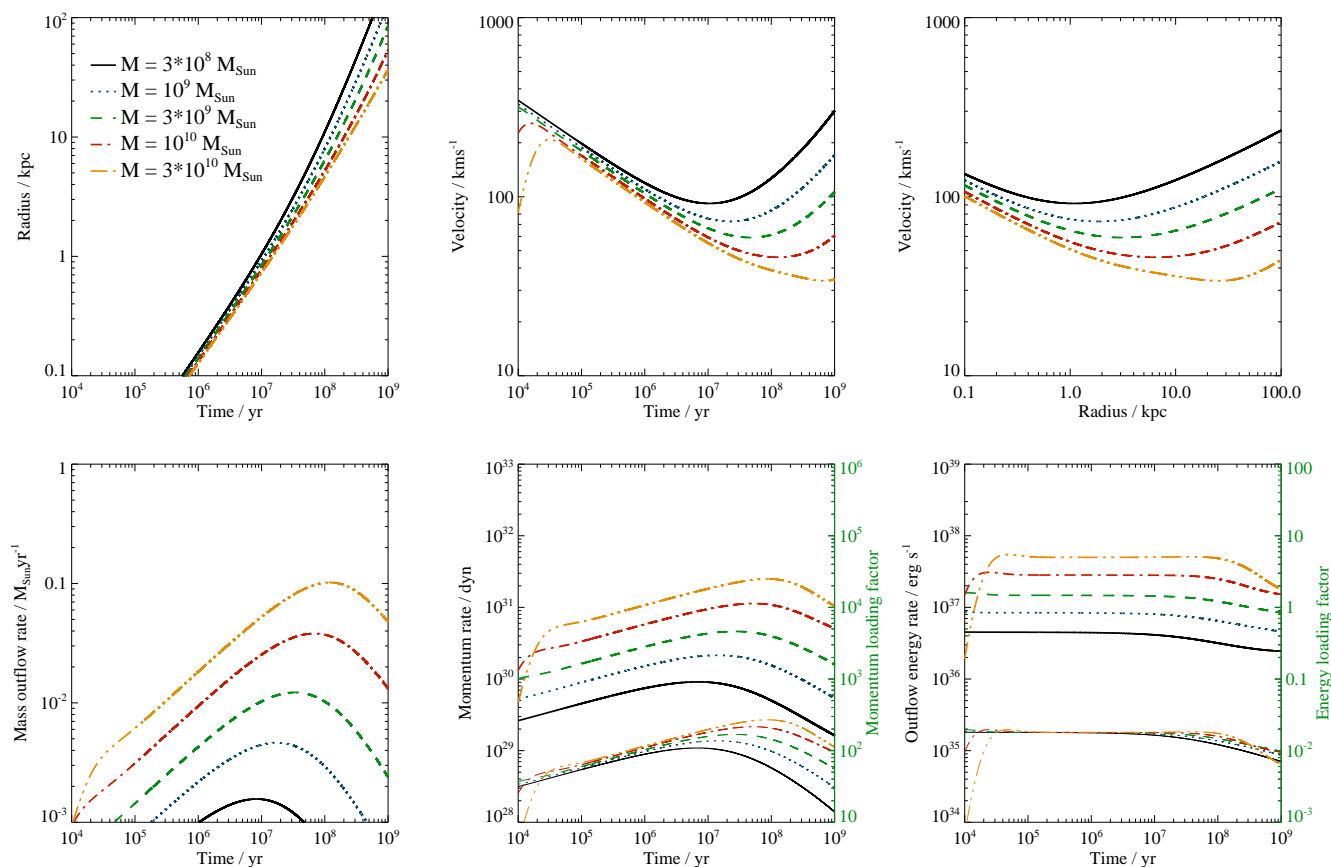


Figure 5. Outflow parameters in simulations with TDE-powered AGN, starting at $z_{\text{init}} = 0.247$, with BH masses linearly proportional to stellar masses and gas mass equal to stellar mass. Panels and lines as in Figure 4.

gas removal by stellar processes is not taken into account; however, some observed galaxies have gas masses close to this limit (Oh et al. 2015; Kirby et al. 2017). In the second case, I use $M_{\text{gas}} = M_*$, which represents a rather drastic case of gas removal, but agrees quite well with the trend in observed dwarf galaxies. The resulting gas masses are given in Table 1.

The initial black hole masses are selected using the black hole mass - stellar mass relation (Reines & Volonteri 2015): $M_{\text{BH}} \simeq 10^{-3.55} M_*$. This results in extremely low black hole masses in the first three cases, $M_{\text{BH},0} < 10^3 M_{\odot}$. However, it turns out that even such tiny black holes are capable of driving outflows, and if the actual black holes were larger, due to the expected rapid growth at high redshift via BH mergers (Devecchi & Volonteri 2009) or direct collapse (Volonteri et al. 2008), the outflows would only be more powerful.

Before presenting the numerical results, I note that it is possible to estimate the expected TDE-powered AGN outflow effect by considering the energy release by the AGN, the binding energy of the gas and the supernova energy injection. These energy values are given in columns 5-7 of Table 1. For supernova energy injection, I assume one supernova per $M_1 \sim 100 M_{\odot}$ of stars formed and $E_1 = 10^{51}$ erg per supernova. The last two columns of the table give ratios E_b/E_{AGN} and $E_{\text{SN}}/E_{\text{AGN}}$, respectively. Given that the fraction of supernova energy communicated to the ISM is $\lesssim 10\%$

(Thornton et al. 1998; Walch & Naab 2015; Fierlinger et al. 2016), and the fraction of AGN energy communicated to the ISM is $\sim 5\%$, it is clear that TDE-powered AGN outflows should be more important than supernovae in the four smallest galaxies, but probably not in the largest one. The total energy input by stellar winds is similar to that of supernovae (Chu 2005; Voss et al. 2009), therefore the relative importance of AGN outflows to stellar feedback is similar when AGN wind feedback is taken into account. Similarly, AGN outflow energy is higher than the gas binding energy in all five gas-poor and three smallest gas-rich models, suggesting that TDE-powered outflows are probably more important in these smallest galaxies. This can be understood by considering that the average AGN luminosity scales as $M_{\text{BH}}^{0.353}$, while BH mass scales approximately as $M_{\text{tot}}^{1.5}$, so $L_{\text{AGN}} \propto M_{\text{tot}}^{0.53}$; on the other hand, the supernova energy release scales as $M_* \propto M_{\text{tot}}^{1.5}$, while the binding energy of the gas scales as M_{tot}^2 . Therefore, the importance of TDE-powered AGN outflows decreases with increasing galaxy mass.

The main results are presented in Figures 4 ($f_b = 0.16$) and 5 ($M_{\text{gas}} = M_*$). In each figure, the six panels show, from left to right and top to bottom, outflow radius against time, velocity against time, velocity against radius, mass outflow rate against time, outflow momentum rate and momentum loading factor $\dot{p}c/L_{\text{AGN}}$ against time, and energy rate and energy conversion efficiency \dot{E}/L_{AGN} against time. Note that the velocity and mass outflow rate scales are dif-

ferent in the two figures. The AGN luminosity used in these comparisons is the average long-term luminosity $\{L_{\text{AGN}}\}$; the actual luminosity during tidal disruption events can be several orders of magnitude higher.

Outflows exist in all models considered here. This is not surprising: assuming a perfectly adiabatic spherically symmetric system, the only possibility of using the injected energy is by gas expansion. It is more important to consider the properties of the outflows and check whether they might be observable. Outflows in gas-rich simulations expand with velocities $10\text{km/s} < v_{\text{out}} < 100\text{km/s}$, which is comparable to the velocity dispersions in real galaxies (Figure 1, middle panel). Therefore such outflows would be difficult to identify, since random gas motions would very easily disrupt the outflow bubble. A large fraction of energy might escape via low-density channels opened by gas turbulence, leading to collapse of any outflow bubble that forms. However, the prolonged AGN energy injection may result in a more radially-dominated velocity anisotropy of gas motions in the galaxy. Formally, outflow radius becomes larger than $r_{\text{eff}} \sim 1\text{ kpc}$ in $< 10^8\text{ yr}$, i.e. the effects of AGN outflows can manifest rather quickly, in a few dynamical times of the galaxy. The mass outflow rate can reach $0.1 - 1M_{\odot}\text{ yr}^{-1}$, a much higher value than typical star formation rates (McGaugh et al. 2017). Therefore gas may be gradually pushed out from the central parts of the galaxy; this can potentially quench star formation to some extent.

In the simulations with low gas density, outflows expand much more rapidly, with $v_{\text{out}} > 100\text{ km/s}$ in the central parts of the galaxy, and all outflows accelerate after passing through the highest circular velocity region of the potential. This should result in outflows that are detectable and might be significant in redistributing the gas in the galaxy. Importantly, in all simulations, outflows reach $r_{\text{out}} = 100\text{ kpc}$ in several Gyr or less, i.e. gas can be removed outside the virial radius of the galaxy. The mass outflow rate is, naturally, much lower than in the high gas density simulations, but even the $10^{-3}M_{\odot}\text{ yr}^{-1} < \dot{M}_{\text{out}} < 0.1M_{\odot}\text{ yr}^{-1}$ rates are comparable to or larger than typical star formation rates in similar galaxies (McGaugh et al. 2017). The integrated mass outflow over the course of the simulation is comparable to the initial gas mass in the galaxy. Therefore, even though the outflow itself might be weak and difficult to detect, perhaps better described as an expanding galactic atmosphere, it might still have a noticeable effect on the host galaxy.

The momentum and kinetic energy rates of outflows in both cases are modest. The momentum loading factors can be very large due to the low outflow velocities ($\dot{p}c/\{L_{\text{AGN}}\} > 10$), but would be much lower if the outflow was detected during a period of nuclear activity following a TDE, because then the momentum rate would be compared with instantaneous, rather than average, AGN luminosity. The same is true of the energy conversion efficiency. Therefore even if an outflow signature is detected in a dwarf galaxy, it might be difficult to connect it to sporadic nuclear activity rather than stellar processes. This has previously been noted in the context of fossil outflows in large galaxies (King et al. 2011; Fluetsch et al. 2018; Nardini & Zubovas 2018).

5 DISCUSSION

5.1 Current and seed black hole masses

The black hole masses used in the calculations of outflow properties are linearly proportional to galaxy stellar masses. If, instead, a lower limit $M_{\text{BH,min}} = 10^3 - 10^4M_{\odot}$ were imposed on the seed SMBH mass, one would expect somewhat stronger outflows in galaxies with $M_{*} \lesssim 5 \times 10^6M_{\odot}$. The outflow velocity scales approximately as $v_{\text{out}} \propto L_{\text{AGN}}^{1/3} \propto M_{\text{BH}}^{0.12}$, while the mass flow rate $\dot{M}_{\text{out}} \propto L_{\text{AGN}}^{1/2} \propto M_{\text{BH}}^{0.18}$; the latter scaling is stronger than predicted by Zubovas & King (2012) because of the radial increase of effective σ in an NFW potential. The outflow kinetic power then scales as $\dot{M}_{\text{out}}v_{\text{out}}^2 \propto M_{\text{BH}}^{0.42}$, i.e. the kinetic power with massive black hole seeds could be as much as 7 – 20 times greater than in galaxies with stellar seeds.

Such outflows would be more easily detectable in the local Universe and might allow checking the hypotheses of SMBH formation. On the other hand, even stellar-mass black holes should grow to $M_f > 10^3M_{\odot}$ by $z = 0$ (see eq. 6), so observations of more distant dwarf galaxies are required in order to be able to distinguish between models of seed black hole masses. As a rough estimate, if we assume that the black hole mass can be determined to within an order of magnitude based on outflow properties, the existence of seed black hole masses $M_{\text{seed}} \gtrsim 10^4M_{\odot}$ can be checked by observing dwarf galaxies at $t \lesssim 10\text{ Gyr}$ after the Big Bang ($z \gtrsim 0.33$), since after that time, a stellar black hole with initial mass $M_0 = 10M_{\odot}$ will have grown to $M_f > 10^3M_{\odot}$. Checking the existence of black holes with $M_{\text{seed}} \gtrsim 10^3M_{\odot}$ would require observing dwarf galaxies at $t \lesssim 2.1\text{ Gyr}$ after the Big Bang ($z \gtrsim 3.1$). Although large numbers of dwarf galaxies with $M_{*} > 10^7M_{\odot}$ are known beyond the Local Volume (e.g. Mezcua et al. 2016, 2018), the faintest dwarfs are so far only found in the Local Universe (Lee et al. 2017). Therefore constraining black hole seed masses using outflow properties is unlikely now, although might become possible in the near future, especially with next generation instruments.

The growth of black holes via TDEs in the smallest galaxies would lead to those black holes becoming overmassive compared to the predictions of black hole - stellar mass correlations. There is a hint that this relation flattens at low masses (Reines & Volonteri 2015, fig. 9), but dynamical measurements of black hole masses in dwarf galaxies are needed before this flattening can be confirmed. If it is, it would provide strong support to the hypothesis that TDEs are an important source of black hole growth in dwarf galaxies.

Another interesting issue is that in the smallest galaxies considered here, the central black hole mass is of the same order as stellar black holes can be, i.e. $M_{\text{BH}} < 100M_{\odot}$. Since even such a small object may create significant outflows in the host galaxy, it is worth considering that several stellar black holes, each powered by independent TDEs, may have an even larger effect on the smallest dwarf galaxies, efficiently driving gas out of the galaxy and leading to the very high observed mass-to-light ratios (Gilmore et al. 2007; Wolf et al. 2010). In this sense, stellar black holes may have a similar effect to ultra-luminous X-ray sources (ULXs; cf. King et al. 2001), except that their feedback would be dis-

tributed in time throughout the age of the galaxy, rather than concentrated around episodes of star formation.

In dwarf galaxies, especially the smallest ones, massive black holes are not necessarily located in the centre: the gravitational potential is so shallow, and the mass ratio between the central object and individual stars so low, that significant black hole wandering can occur (Bellovary et al. 2018). This process would lead to highly asymmetric disturbances to galactic gas after each TDE and associated activity episode. This may perhaps explain some puzzling features in dwarf galaxies, e.g. the wide holes in the gas distributions in Leo A and Aquarius (Hunter et al. 2012).

5.2 Observability of TDE-driven outflows

The energies released by TDEs in dwarf galaxies are typically higher than gas binding energies or supernova energy release (see Table 1), even accounting for the 5% coupling efficiency of this energy to the ISM. However, outflows produced by TDE-powered AGN don't always break out of galaxies and will not generally be easily detectable due to their low velocities (see Section 4.3 and Figures 4 and 5). Therefore, the AGN energy input may manifest differently, for example, by creating a slowly expanding gaseous 'atmosphere' or by increasing gas turbulence in the galaxy. These effects can be detected by observing gas kinematics and density profiles. In the long run, this process may significantly decrease the star formation efficiency in dwarf galaxies. This may explain the low observed star formation efficiency (McGaugh et al. 2017). In galaxy samples selected by dynamical mass, differences in stellar mass would then correlate with presence of central massive black holes.

On shorter timescales, disturbances of dwarf galaxy ISM should persist for at least an order magnitude longer than the AGN episode that drove the outflow (King et al. 2011). Therefore, we can expect $\sim 10\%$ of dwarf galaxies that harbour massive black holes to show disturbances in their ISM. This number can be used to estimate SMBH occupancy fraction in dwarf galaxies. More detailed numerical simulations, which are beyond the scope of this paper, would help predict the expected effects in more detail and could be tested with spatially resolved dwarf galaxy observations, which will be provided by, e.g., the Euclid space observatory (Laureijs et al. 2011).

As each TDE lasts for only $t \lesssim 100$ yr, the effects of individual activity episodes may be visible to some extent in the galaxy. The outer edge of the expanding atmosphere or zone of increased turbulence (see above) moves with the low average velocity (Section 4.3), but each individual episode can create a faster shell propagating inside this zone. The speed on individual shells is $v_{\text{ind}}/v_{\text{out}} \simeq (L_{\text{AGN}}/\langle L_{\text{AGN}} \rangle)^{1/3} \simeq f_{\text{AGN}}^{-1/3} \sim 5$. In almost all the cases considered in this paper, this leads to outflows moving with velocities $v_{\text{ind}} > 100 \text{ km s}^{-1}$, and sometimes with $v_{\text{ind}} > 10^3 \text{ km s}^{-1}$. Such individual outflow shells would be easily detectable. The most important caveat here is that the properties of the shell motion do not depend strongly on the AGN feeding source, therefore AGN fed by gas streams should cause essentially identical outflows. The presence of gas moving with high radial velocities is therefore evidence of an AGN episode in the recent past, rather than evidence of

the AGN feeding mechanism. The presence of multiple shell moving with different radial velocities, however, may signal that there have been several individual AGN episodes in the recent past, which is more likely if the episodes are triggered by TDEs than if they are fed by large gas streams. Detection of individual shells requires spatially-resolved spectra of dwarf galaxies, but this may be possible in the near future.

Shells expanding through the turbulent ISM of the dwarf galaxy would be subject to various instabilities, most notably the Rayleigh-Taylor and Richtmyer-Meshkov instabilities due to impacts with the surrounding ISM, and Vishniac instability (Vishniac 1983) due to density increase and self-gravity. The compaction of ISM and the increased mixing of material with different orbital energies and angular momenta can in fact lead to enhancement of SMBH accretion via gas streams (Dehnen & King 2013). In this way, TDE-powered AGN outflows can kick-start the process of SMBH growth in dwarf galaxies. Magnetic fields can prevent the growth of instabilities (Diehl et al. 2008), but are unlikely to be very efficient, since dwarf galaxies tend to have weaker magnetic fields than larger ones (Chyży et al. 2011).

Finally, the repeated shell expansion and contraction due to individual TDE-powered AGN episodes may lead to a relaxation of the central dark matter cusp, as seen in simulations of repeated supernova feedback (Pontzen & Governato 2012; Governato et al. 2012). This process, therefore, may help solve the cusp-core problem in dwarf galaxies, as suggested by Silk (2017).

5.3 Enhancement of star formation rates

In the gas-rich galaxy simulations, outflow pressure peaks at $\sim 10^4 - 10^5 \text{ yr}$, at a few times 10^7 K cm^{-3} , and then decreases as a power law with time. Assuming an ISM pressure $P_{\text{ISM}}/k_{\text{B}} = 10^5 \text{ K cm}^{-3}$ (Young et al. 2001), the outflow pressure exceeds the ISM pressure for a few Myr. Therefore, at very early times, outflowing gas might compress denser clumps in the ISM and enhance the star formation rate (Silk 2005; Zubovas et al. 2014; Zubovas & King 2016). This should not be a significant effect: even assuming that the whole star-forming ISM is affected and that the star formation rate increases linearly with pressure enhancement, the expected SFR increase will not exceed a factor $R_{\text{SFR}} \sim 100$. Given that the specific star formation rate in galaxies is $< 10^{-8} \text{ yr}^{-1}$, even at high redshift (Behroozi et al. 2013), the triggered star formation can only lead to a stellar mass increase of $10^{-8} \text{ yr}^{-1} \cdot R_{\text{SFR}} \cdot 10^6 \text{ yr} \sim 1$ times the natural star formation. In other words, the outflow-triggered star formation can be responsible for at most 50% of the star formation in the first 100 Myr of the dwarf galaxy's evolution. Detecting such differences would require very precise determination of the star formation history and initial conditions of the dwarf galaxy.

5.4 Other modes of feedback

One more complication to understanding the growth on SMBHs in dwarf galaxies is feeding by gas streams. Even though it is unlikely to contribute much to black hole growth (see Section 2), this process can still occur occasionally,

feed the black hole and affect the host galaxy significantly. Dashyan et al. (2018) investigated the possibility of AGN outflows in dwarf galaxies while treating the AGN luminosity as a free parameter, and found that AGN feedback can be more powerful than supernova feedback, if the AGN are fed at high Eddington ratios and/or if the supernova wind coupling efficiency is low. These results are qualitatively similar to those presented here, since TDE-powered AGN can also have phases of high Eddington ratio accretion. One drawback of that study is that the pdV work done by the expanding gas, which accounts for $\sim 1/3$ of the injected AGN wind energy (Zubovas & King 2012), was not included in the outflow energy equation (their eq. 7), so the actual AGN outflow powers should be smaller than presented there.

It is now established that TDEs can launch jets from the accretion disc (Levan et al. 2011; Burrows et al. 2011; Cenko et al. 2012; Komossa 2015). The luminosity of the jet can, at least initially, be much higher than that of the disc (Piran et al. 2015). However, the duration of peak jet activity is of order of weeks or months (Mimica et al. 2015), much less than the lifetime of the accretion disc built up during a TDE (see Section 3.2). Therefore the importance of the jet on long timescales is most likely small. In addition, the major effects of jets should be confined to sub-parsec scales and manifest on several year timescales (Giannios & Metzger 2011). Even if the jet is energetically important, its overall effect may be similar to that of a wide-angle wind-driven outflow, since the jet may inflate a bubble in the host galaxy and affect its ISM throughout the host (e.g., Gaibler et al. 2012).

5.5 Validity of TDE rates

The TDE rates used in this work are theoretical estimates which are based on rather idealized assumptions regarding the distribution of stars in the galaxy. Some processes, for example the presence of circumnuclear stellar rings and eccentricity oscillations therein, may raise the TDE rate, possibly significantly (Madigan et al. 2018). Other processes might reduce the rate: for example, the TDE rate extrapolated from the results of Stone & Metzger (2016) to the smallest galaxies results in most of the stellar population being disrupted over the Hubble time. This is unlikely to be the case, and in such galaxies, the calculation of TDE rates should take into account the finite amount of available stars, leading to a lower estimate (for example, as in numerical simulations by Brockamp et al. 2011). Nevertheless, it is interesting to note that the decrease of stellar mass due to TDEs might contribute to the very high mass-to-light ratios in the smallest galaxies (Gilmore et al. 2007; Wolf et al. 2010; Read et al. 2017).

Observational estimates of the true rates of tidal disruption events are also difficult to make. Many theoretical predictions might be overestimates by as much as an order of magnitude (see discussion in Stone & Metzger 2016). However, a broad range $\dot{N}_{\text{TDE}} \sim 10^{-5} - 10^{-4} \text{ yr}^{-1}$ per galaxy, given in a review by Komossa (2015), falls within the range used in this work for $M_{\text{BH}} > 1.9 \times 10^4 M_{\odot}$, which is consistent with the mass range for which observational constraints are available. The true rate might even be somewhat higher than these observations suggest, for two reasons. Highly super-Eddington TDEs may not follow the canonical

$t^{-5/3}$ luminosity profile due to accretion being limited by viscous transport (Lin et al. 2017; Wu et al. 2018) and therefore might not always be identified as such. Secondly, TDEs around the smallest black holes may be more difficult to detect because their peak luminosity is smaller (De Colle et al. 2012), and because the probability of prompt emission, with a different light curve, resulting from direct impact by the star becomes non-negligible, since the tidal disruption radius becomes only a few times the stellar radius.

Overall, if the actual TDE rate is significantly lower than that calculated by Stone & Metzger (2016), then TDE-powered AGN and their associated outflows are much rarer than predicted here, and would be unable to explain the observed population of AGN in dwarf galaxies. If the actual TDE rate is higher, then the predicted AGN fraction in dwarf galaxies is also higher and implies that not all dwarf galaxies harbour massive central black holes. In either case, future theoretical work and better observational constraints will help determine the frequency of TDEs and the occupation fraction of massive black holes in dwarf galaxies.

6 SUMMARY AND CONCLUSIONS

I have investigated the possibility of powering AGN by tidal disruption events and of such AGN driving outflows in dwarf galaxies. The results, based on analytical arguments and numerical calculations of outflow properties, are the following:

- TDEs can feed supermassive black holes in dwarf galaxies, producing mass inflow rates large enough for AGN episodes to last, in total, for a significant fraction ($\gtrsim 1\%$) of Hubble time.
- Accounting for the viscous timescale of matter infall suggests that each dwarf galaxy hosting a SMBH can be active for an even larger fraction of the Hubble time.
- The total energy released by TDE-powered accretion episodes in a galaxy with $10^5 M_{\odot} < M_{*} < 10^8 M_{\odot}$ is larger than the total energy released by supernovae or the binding energy of the gas in the same galaxy.
- Outflows driven by TDE-powered AGN can break out of the smallest gas-rich dwarf galaxies and out of most gas-poor dwarf galaxies.
- The velocities of outflows driven by TDE-powered AGN in gas-rich dwarf galaxies are small, making these outflows difficult to detect; instead, their effects might be observable as increased turbulence and extended gas distribution.

As more data of AGN in dwarf galaxies, as well as spatially resolved dwarf galaxies, become available, the predictions presented here may be tested and used to constrain the occupancy fraction of massive black holes in dwarf galaxies, as well as the actual effects they have on the evolution of their hosts.

ACKNOWLEDGMENTS

I thank Chris Nixon for comments and suggestions during the preparation of this manuscript, and the anonymous referee for insightful comments that helped put the findings presented here in their proper context. This research was funded by a grant (No. LAT-09/2016) from the Research Council of Lithuania.

REFERENCES

- Ann H. B., 2017, *Journal of Korean Astronomical Society*, 50, 111
- Behroozi P. S., Wechsler R. H., Conroy C., 2013, *ApJ*, 770, 57
- Bellovary J., Cleary C., Munshi F., Tremmel M., Christensen C., Brooks A., Quinn T., 2018, *ArXiv e-prints*
- Bonoli S., Mayer L., Kazantzidis S., Madau P., Bellovary J., Governato F., 2016, *MNRAS*, 459, 2603
- Brockamp M., Baumgardt H., Kroupa P., 2011, *MNRAS*, 418, 1308
- Bryan G. L., Norman M. L., 1998, *ApJ*, 495, 80
- Burrows D. N., Kennea J. A., Ghisellini G., Mangano V., Zhang B., Page K. L., Eracleous M., Romano P., et al. 2011, *Nature*, 476, 421
- Cenko S. B., Krimm H. A., Horesh A., Rau A., Frail D. A., Kennea J. A., Levan A. J., Holland S. T., et al. 2012, *ApJ*, 753, 77
- Chilingarian I. V., Katkov I. Y., Zolotukhin I. Y., Grishin K. A., Beletsky Y., Boutsia K., Osip D. J., 2018, *ArXiv e-prints*
- Chu Y.-H., 2005, in Braun R., ed., *Extra-Planar Gas Vol. 331 of Astronomical Society of the Pacific Conference Series, Quantifying Stellar Energy Feedback*. p. 297
- Chyży K. T., Weżgowiec M., Beck R., Bomans D. J., 2011, *A&A*, 529, A94
- Coker R. F., Melia F., 1997, *ApJL*, 488, L149
- Coughlin E. R., Nixon C., 2015, *ApJL*, 808, L11
- Coughlin E. R., Nixon C., Begelman M. C., Armitage P. J., Price D. J., 2016, *MNRAS*, 455, 3612
- Cuadra J., Nayakshin S., Martins F., 2008, *MNRAS*, 383, 458
- Cuadra J., Nayakshin S., Springel V., Di Matteo T., 2005, *MNRAS*, 360, L55
- Cuadra J., Nayakshin S., Wang Q. D., 2015, *MNRAS*, 450, 277
- Cummings J. D., Kalirai J. S., Tremblay P.-E., Ramirez-Ruiz E., Choi J., 2018, *ApJ*, 866, 21
- Dashyan G., Silk J., Mamon G. A., Dubois Y., Hartwig T., 2018, *MNRAS*, 473, 5698
- Davies R., Burtscher L., Dodds-Eden K., Orban de Xivry G., 2012, in *Journal of Physics Conference Series Vol. 372 of Journal of Physics Conference Series, Do stellar winds play a decisive role in feeding AGN?*. p. 012046
- Davies R. I., Müller Sánchez F., Genzel R., Tacconi L. J., Hicks E. K. S., Friedrich S., Sternberg A., 2007, *ApJ*, 671, 1388
- De Colle F., Guillochon J., Naiman J., Ramirez-Ruiz E., 2012, *ApJ*, 760, 103
- Dehnen W., King A., 2013, *ApJL*, 777, L28
- Devecchi B., Volonteri M., 2009, *ApJ*, 694, 302
- Diehl S., Li H., Fryer C. L., Rafferty D., 2008, *ApJ*, 687, 173
- Dutton A. A., Macciò A. V., 2014, *MNRAS*, 441, 3359
- Eftekhari T., Berger E., Zauderer B. A., Margutti R., Alexander K. D., 2018, *ApJ*, 854, 86
- Faucher-Giguère C.-A., Quataert E., 2012, *MNRAS*, 425, 605
- Ferrarese L., Côté P., Dalla Bontà E., Peng E. W., Merritt D., Jordán A., Blakeslee J. P., Hasegan M., Mei S., Piatek S., Tonry J. L., West M. J., 2006, *ApJL*, 644, L21
- Fierlinger K. M., Burkert A., Ntormousi E., Fierlinger P., Schartmann M., Ballone A., Krause M. G. H., Diehl R., 2016, *MNRAS*, 456, 710
- Finlator K., Davé R., 2008, *MNRAS*, 385, 2181
- Fluetsch A., Maiolino R., Carniani S., Marconi A., Cicone C., Bourne M. A., Costa T., Fabian A. C., Ishibashi W., Venturi G., 2018, *ArXiv e-prints*
- Gaibler V., Khochfar S., Krause M., Silk J., 2012, *MNRAS*, 425, 438
- Gezari S., Chornock R., Rest A., Huber M. E., Forster K., Berger E., Challis P. J., Neill J. D., et al. 2012, *Nature*, 485, 217
- Giannios D., Metzger B. D., 2011, *MNRAS*, 416, 2102
- Gilmore G., Wilkinson M. I., Wyse R. F. G., Kleya J. T., Koch A., Evans N. W., Grebel E. K., 2007, *ApJ*, 663, 948
- Governato F., Zolotov A., Pontzen A., Christensen C., Oh S. H., Brooks A. M., Quinn T., Shen S., Wadsley J., 2012, *MNRAS*, 422, 1231
- Graham A. W., 2016, in Laurikainen E., Peletier R., Gadotti D., eds, *Galactic Bulges Vol. 418 of Astrophysics and Space Science Library, Galaxy Bulges and Their Massive Black Holes: A Review*. p. 263
- Greene J. E., Barth A. J., Ho L. C., 2006, *New Astron. Rev.*, 50, 739
- Habouzit M., Volonteri M., Dubois Y., 2017, *MNRAS*, 468, 3935
- Hayasaki K., Stone N., Loeb A., 2013, *MNRAS*, 434, 909
- Heckman T. M., Best P. N., 2014, *ARA&A*, 52, 589
- Holoien T. W.-S., Kochanek C. S., Prieto J. L., Grupe D., Chen P., Godoy-Rivera D., Stanek K. Z., Shappee B. J., et al. 2016, *MNRAS*, 463, 3813
- Hunter D. A., Ficut-Vicas D., Ashley T., Brinks E., Cigan P., Elmegreen B. G., Heesen V., Herrmann K. A., Johnson M., Oh S.-H., Rupen M. P., Schruha A., Simpson C. E., Walter F., Westpfahl D. J., Young L. M., Zhang H.-X., 2012, *AJ*, 144, 134
- Igarashi A., Mori M., Nitta S.-y., 2017, *MNRAS*, 470, 2225
- Inayoshi K., Haiman Z., Ostriker J. P., 2016, *MNRAS*, 459, 3738
- Iorio G., Fraternali F., Nipoti C., Di Teodoro E., Read J. I., Battaglia G., 2017, *MNRAS*, 466, 4159
- Kallivayalil N., van der Marel R. P., Alcock C., 2006, *ApJ*, 652, 1213
- King A., Lasota J.-P., 2016, *MNRAS*, 458, L10
- King A., Nixon C., 2015, *MNRAS*, 453, L46
- King A. R., 2010, *MNRAS*, 402, 1516
- King A. R., Davies M. B., Ward M. J., Fabbiano G., Elvis M., 2001, *ApJL*, 552, L109
- King A. R., Pounds K. A., 2003, *MNRAS*, 345, 657
- King A. R., Zubovas K., Power C., 2011, *MNRAS*, 415, L6
- Kirby E. N., Rizzi L., Held E. V., Cohen J. G., Cole A. A., Manning E. M., Skillman E. D., Weisz D. R., 2017, *ApJ*, 834, 9
- Komossa S., 2015, *Journal of High Energy Astrophysics*, 7, 148
- Kourkchi E., Khosroshahi H. G., Carter D., Karick A. M., Mármol-Queraltó E., Chiboucas K., Tully R. B., Mobasher B., Guzmán R., Matković A., Gruel N., 2012, *MNRAS*, 420, 2819
- Laureijs R., Amiaux J., Arduini S., Auguères J., Brinchmann J., Cole R., Cropper M., Dabin C., Duvet L., Ealet A., et al. 2011, *ArXiv e-prints*

- Lee M. G., Jang I. S., Beaton R., Seibert M., Bono G., Madore B., 2017, *ApJL*, 835, L27
- Leitherer C., Robert C., Drissen L., 1992, *ApJ*, 401, 596
- Levan A. J., Tanvir N. R., Cenko S. B., Perley D. A., Wiersema K., Bloom J. S., Fruchter A. S., Postigo A. d. U., et al. 2011, *Science*, 333, 199
- Lin D., Guillochon J., Komossa S., Ramirez-Ruiz E., Irwin J. A., Maksym W. P., Grupe D., Godet O., Webb N. A., Barret D., Zauderer B. A., Duc P.-A., Carrasco E. R., Gwyn S. D. J., 2017, *Nature Astronomy*, 1, 0033
- Lodato G., King A. R., Pringle J. E., 2009, *MNRAS*, 392, 332
- Lu W., Kumar P., 2018, *ArXiv e-prints*
- Madigan A.-M., Halle A., Moody M., McCourt M., Nixon C., Wernke H., 2018, *ApJ*, 853, 141
- Mageshwaran T., Mangalam A., 2018, *ArXiv e-prints*
- Magorrian J., Tremaine S., 1999, *MNRAS*, 309, 447
- Martin-Navarro I., Mezcua M., 2018, *ArXiv e-prints*
- McGaugh S. S., Schombert J. M., Lelli F., 2017, *ApJ*, 851, 22
- McNamara B. R., Nulsen P. E. J., 2007, *ARA&A*, 45, 117
- Mezcua M., 2017, *International Journal of Modern Physics D*, 26, 1730021
- Mezcua M., Civano F., Fabbiano G., Miyaji T., Marchesi S., 2016, *ApJ*, 817, 20
- Mezcua M., Civano F., Marchesi S., Suh H., Fabbiano G., Volonteri M., 2018, *MNRAS*
- Mimica P., Giannios D., Metzger B. D., Aloy M. A., 2015, *MNRAS*, 450, 2824
- Nardini E., Zubovas K., 2018, *MNRAS*
- Nayakshin S., Wilkinson M. I., King A., 2009, *MNRAS*, 398, L54
- Oh S.-H., Hunter D. A., Brinks E., Elmegreen B. G., Schrubba A., Walter F., Rupen M. P., Young L. M., Simpson C. E., Johnson M. C., Herrmann K. A., Ficut-Vicas D., Cigan P., Heesen V., Ashley T., Zhang H.-X., 2015, *AJ*, 149, 180
- Pardo K., Goulding A. D., Greene J. E., Somerville R. S., Gallo E., Hickox R. C., Miller B. P., Reines A. E., Silverman J. D., 2016, *ApJ*, 831, 203
- Penny S. J., Masters K. L., Smethurst R., Nichol R. C., Krawczyk C. M., Bizyaev D., Greene O., Liu C., Marinelli M., Rembold S. B., Riffel R. A., Ilha G. d. S., Wylezalek D., Andrews B. H., Bundy K., Drory N., Oravetz D., Pan K., 2018, *MNRAS*, 476, 979
- Piran T., Sądowski A., Tchekhovskoy A., 2015, *MNRAS*, 453, 157
- Piran T., Svirski G., Krolik J., Cheng R. M., Shiokawa H., 2015, *ApJ*, 806, 164
- Planck Collaboration Ade P. A. R., Aghanim N., Arnaud M., Ashdown M., Aumont J., Baccigalupi C., Banday A. J., Barreiro R. B., Bartlett J. G., et al. 2016, *A&A*, 594, A13
- Pontzen A., Governato F., 2012, *MNRAS*, 421, 3464
- Pounds K. A., Reeves J. N., King A. R., Page K. L., O'Brien P. T., Turner M. J. L., 2003, *MNRAS*, 345, 705
- Ramirez-Ruiz E., Rosswog S., 2009, *ApJL*, 697, L77
- Read J. I., Iorio G., Agertz O., Fraternali F., 2017, *MNRAS*, 467, 2019
- Rees M. J., 1988, *Nature*, 333, 523
- Reines A. E., Volonteri M., 2015, *ApJ*, 813, 82
- Sakurai Y., Yoshida N., Fujii M. S., 2018, *ArXiv e-prints*
- Schawinski K., Koss M., Berney S., Sartori L. F., 2015, *MNRAS*, 451, 2517
- Schaye J., Dalla Vecchia C., Booth C. M., Wiersma R. P. C., Theuns T., Haas M. R., Bertone S., Duffy A. R., McCarthy I. G., van de Voort F., 2010, *MNRAS*, 402, 1536
- Shakura N. I., Sunyaev R. A., 1973, *A&A*, 24, 337
- Shankar F., Lapi A., Salucci P., De Zotti G., Danese L., 2006, *ApJ*, 643, 14
- Sharma M., Nath B. B., 2013, *ApJ*, 763, 17
- Shull J. M., 1983, *ApJ*, 264, 446
- Silk J., 2005, *MNRAS*, 364, 1337
- Silk J., 2017, *ApJL*, 839, L13
- Stone N. C., Metzger B. D., 2016, *MNRAS*, 455, 859
- Thornton K., Gaudlitz M., Janka H.-T., Steinmetz M., 1998, *ApJ*, 500, 95
- Toloba E., Guhathakurta P., Peletier R. F., Boselli A., Lisker T., Falcón-Barroso J., Simon J. D., van de Ven G., et al. 2014, *ApJS*, 215, 17
- Tombesi F., Cappi M., Reeves J. N., Palumbo G. G. C., Yaqoob T., Braitto V., Dadina M., 2010a, *A&A*, 521, A57+
- Tombesi F., Sambruna R. M., Reeves J. N., Braitto V., Ballo L., Gofford J., Cappi M., Mushotzky R. F., 2010b, *ApJ*, 719, 700
- Trebitsch M., Volonteri M., Dubois Y., Madau P., 2017, *ArXiv e-prints*
- van der Marel R. P., Alves D. R., Hardy E., Suntzeff N. B., 2002, *AJ*, 124, 2639
- Vishniac E. T., 1983, *ApJ*, 274, 152
- Volonteri M., 2012, *Science*, 337, 544
- Volonteri M., Lodato G., Natarajan P., 2008, *MNRAS*, 383, 1079
- Voss R., Diehl R., Hartmann D. H., Cerviño M., Vink J. S., Meynet G., Limongi M., Chieffi A., 2009, *A&A*, 504, 531
- Walch S., Naab T., 2015, *MNRAS*, 451, 2757
- Walker M. G., Mateo M., Olszewski E. W., Peñarrubia J., Wyn Evans N., Gilmore G., 2009, *ApJ*, 704, 1274
- Wang J., Merritt D., 2004, *ApJ*, 600, 149
- Weisz D. R., Dolphin A. E., Skillman E. D., Holtzman J., Gilbert K. M., Dalcanton J. J., Williams B. F., 2014, *ApJ*, 789, 147
- Willson L. A., 2000, *ARA&A*, 38, 573
- Wolf J., Martinez G. D., Bullock J. S., Kaplinghat M., Geha M., Muñoz R. R., Simon J. D., Avedo F. F., 2010, *MNRAS*, 406, 1220
- Wu S., Coughlin E. R., Nixon C., 2018, *MNRAS*
- Yang G., Brandt W. N., Vito F., Chen C.-T. J., Trump J. R., Luo B., Sun M. Y., Xue Y. Q., Koekemoer A. M., Schneider D. P., Vignali C., Wang J.-X., 2018, *MNRAS*, 475, 1887
- Yang G., Chen C.-T. J., Vito F., Brandt W. N., Alexander D. M., Luo B., Sun M. Y., Xue Y. Q., Bauer F. E., Koekemoer A. M., Lehmer B. D., Liu T., Schneider D. P., Shemmer O., Trump J. R., Vignali C., Wang J.-X., 2017, *ApJ*, 842, 72
- Young L. M., van Zee L., Dohm-Palmer R. C., Lo K. Y., 2001, in Hibbard J. E., Rupen M., van Gorkom J. H., eds, *Gas and Galaxy Evolution Vol. 240 of Astronomical Society of the Pacific Conference Series, Star Formation and the Interstellar Medium in Dwarf Galaxies*. p. 187
- Zubovas K., King A., 2012, *ApJL*, 745, L34
- Zubovas K., King A., 2016, *MNRAS*, 462, 4055

- Zubovas K., King A. R., Nayakshin S., 2011, MNRAS, 415, L21
Zubovas K., Nayakshin S., King A., Wilkinson M., 2013, MNRAS, 433, 3079
Zubovas K., Sabulis K., Naujalis R., 2014, MNRAS, 442, 2837